

BEAM-PRESENT ANALYSIS OF DISC-LOADED-COAXIAL WAVEGUIDE FOR APPLICATION IN GYRO-TWT (PART-2)

V. Kesari

Microwave Tube Research and Development Centre
Bangalore-13, India

Abstract—The earlier developed combined beam-absent analysis of the disc-loaded-coaxial waveguide in two-configurations (part-1) has shown promise for wideband gyro-traveling-wave tube (gyro-TWT) if the configurations are used as interaction structure. In the present paper, the beam-present dispersion relation and small-signal gain equation in Pierce's format for the disc-loaded-coaxial waveguide were developed. A broadening of the device bandwidth was presented by disc-loading the coaxial waveguide interaction structure of a gyro-TWT with a comparison against the circular cylindrical waveguide, coaxial waveguide, and disc-loaded circular waveguide in their respective gain-frequency responses obtained by using a numerical computer code on the basis of the present beam-present analysis.

1. INTRODUCTION

Beam-absent or cold analysis developed in the preceding paper (part-1), which in turn gives the dispersion and azimuthal interaction impedance characteristics of the disc-loaded-coaxial waveguide, is helpful in characterizing the interaction structure of a gyro-TWT with the metal loading in two configurations. Thus, one may optimize the structure parameters for the desired shape of the dispersion characteristics at relatively higher azimuthal interaction impedance, which has relevance to the device gain. However, to explore the potential of the considered structure loading, not only the beam-absent analysis, but also the hot or beam-present analysis, which would yield the gain-frequency response of the device, needs to be developed.

In the past, the beam-present small signal analyses were developed for various interaction structures for the fast- [1–9] and slow- [10–13] traveling-wave devices. For the purpose of developing the gain-frequency response of the present case of gyro-TWT, as done in the past, with reference to dielectric-loaded [1, 2] or helix-loaded [3] or metal vane-loaded [4] or annular disc-loaded [5, 6] gyro-TWTs, the propagation constant predicted by the beam-absent analysis of the loaded structure was substituted into the beam-present dispersion relation of a gyro-TWT in an unloaded or smooth-wall structure, which is subsequently interpreted for the device gain. Hence, the small-signal analysis of a gyro-TWT in a simple smooth-wall circular waveguide excited in the TE mode was reviewed [1–6]. In a similar way, in the present paper, for the two configurations, not only the propagation constant predicted by the beam-absent analysis of the loaded structure but also the EM field components, satisfied with relevant boundary conditions, are considered in the beam-present analysis. The analysis leads to the hot or beam-present dispersion relation of a gyro-TWT (Section 2) and, subsequently, the device gain (Section 3). Finally, the axial phase propagation constant with reference to the two configurations, obtainable from its beam-absent analysis (part-1), is fed into the gain equation as an input to obtain the gain-frequency response of a gyro-TWT (Section 4), and the study is concluded (Section 5).

2. BEAM-PRESENT DISPERSION RELATION

In a small-orbit gyro-TWT device model, there are a number of thin hollow electron beams of monoenergetic electrons following helical trajectories, all with the same Larmor radius r_L (say), such that their guiding centres are located on a common guiding circle of radius r_H (say), referred as the hollow beam radius, and the centre of the guiding circle lies on the axis of the circular cylindrical interaction structure. Thus, one may consider $2r_L$ as the radial beam thickness. Taking the cylindrical coordinate (r, θ, z) system, for a circular waveguide, excited in the TE mode ($E_z = 0; H_z \neq 0$), the wave equation for $B_z (= \mu_0 H_z)$ in vicinity of such an electron beam, may be written as [1, 6–9]:

$$\frac{\partial^2 B_z}{\partial r^2} + \frac{1}{r} \frac{\partial B_z}{\partial r} + \frac{1}{r^2} \frac{\partial^2 B_z}{\partial \theta^2} + \frac{\partial^2 B_z}{\partial z^2} - \mu_0 \epsilon_0 \frac{\partial^2 B_z}{\partial t^2} = -\frac{1}{r} \left(\frac{\partial}{\partial r} (r J_\theta) - \frac{\partial J_r}{\partial \theta} \right) \quad (1)$$

where J_θ and J_r refer to the azimuthal and the radial components of current density, respectively.

One may consider negligible perturbation of the radial and axial fields in the circular waveguide due to hollow electron beam. In that

case, the solution of wave Equation (1) with its right hand side dropped would give the field dependence. One may represent (1), using such field dependence and the recurrence relation of Bessel functions and their derivatives [7], as

$$(k^2 - \beta^2 - k_t^2)B_z = -\frac{\mu_0}{r} \left(\frac{\partial}{\partial r}(rJ_\theta) - \frac{\partial J_r}{\partial \theta} \right) \quad (2)$$

where β and k_t have now to be interpreted, respectively, as the axial and the transverse propagation constants of the beam-wave coupled system representing the device.

One may express B_z under the zero tangential component of electric field intensities at the metal boundaries (surfaces of waveguide-inner-wall ($r = r_W$) and coaxial-rod ($r = r_C$)), for azimuthally symmetric ($\partial/\partial\theta = 0$) mode, as

$$B_z = B_{z0}Z_0\{k_t r\} \exp j(\omega t - \beta z) \quad (3)$$

where B_{z0} is the amplitude of axial magnetic flux density; and

$$Z_0\{k_t r\} = \left\{ \begin{array}{ll} J_0\{k_t r\} - \frac{J'_0\{k_t r_C\}}{Y'_0\{k_t r_C\}} Y_0\{k_t r\} & \text{Conf.-A} \\ J_0\{k_t r\} - \frac{J'_0\{k_t r_W\}}{Y'_0\{k_t r_W\}} Y_0\{k_t r\} & \text{Conf.-B} \end{array} \right\},$$

r_C and r_W being radii of the coaxial-insert and waveguide, respectively (Fig. 1).

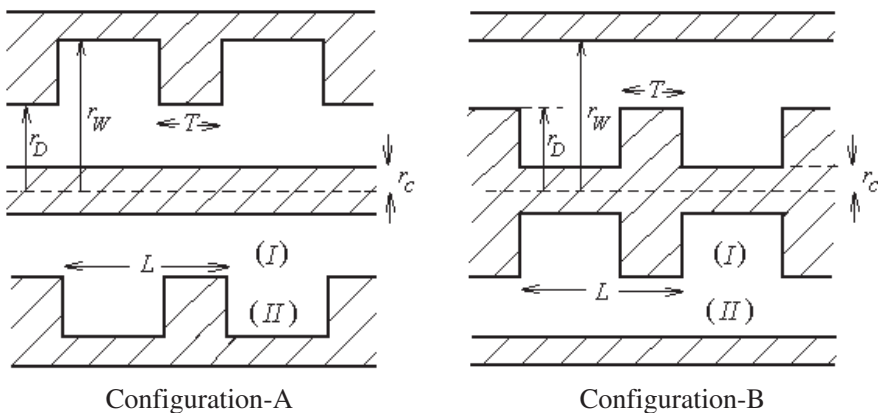


Figure 1. Longitudinal-view of disc-loaded-coaxial waveguide with metal discs radially projecting inward and outward from the metallic envelope (Configuration-A) and from the coaxial insert (Configuration-B), respectively. (Recast after previous paper (Part-1).

Substituting B_z from (3) into (2), multiplying the latter by $rZ_0\{k_t r\}$, then integrating over the free-space guide cross-section ($r_X \leq r \leq r_Y$) (where for Configuration-A: $r_X = r_C$ and $r_Y = r_D$, and for Configuration-B: $r_X = r_D$ and $r_Y = r_W$), and using Lommel's integral [14], one obtains

$$(k^2 - \beta^2 - k_t^2)\chi B_{z0} \exp(\omega t - \beta z) = -\mu_0 \int_{r=r_X}^{r_Y} \left(\frac{\partial}{\partial r}(rJ_\theta) - \frac{\partial J_r}{\partial \theta} \right) Z_0\{k_t r\} dr, \quad (4)$$

where

$$\chi = \frac{r_Y^2}{2} \left(Z_0'^2\{k_t r_Y\} + Z_0^2\{k_t r_Y\} \right) - \frac{r_X^2}{2} \left(Z_0'^2\{k_t r_X\} + Z_0^2\{k_t r_X\} \right),$$

that is

$$\chi = \begin{cases} (r_D^2/2)[Z_0'^2\{k_t r_D\} + Z_0^2\{k_t r_D\}] - (r_C^2/2)Z_0^2\{k_t r_C\} & \text{Conf.-A} \\ (r_W^2/2)Z_0^2\{k_t r_W\} - (r_D^2/2)(Z_0'^2\{k_t r_D\} + Z_0^2\{k_t r_D\}) & \text{Conf.-B} \end{cases};$$

r_D being the radius of disc-hole (Configuration-A) and the outer radius of disc (Configuration-B) (Fig. 1).

Equation (4) consisting of a definite integral in the radial space of the waveguide is a non-explicit form of the dispersion relation of a gyro-TWT, which may be written in an explicit form by first evaluating J_θ and J_r in the integrand of (4) from the dynamics of beam electrons described by the relativistic Vlasov equation [7–9, 15], and then evaluating the integral, as explained in an appendix through intermediate steps (Appendix). That allows one to express (4) in the following explicit form of the dispersion relation of a gyro-TWT:

$$k^2 - \beta^2 - k_t^2 = \frac{-\mu_0 |e|^2 N_0}{2\chi\gamma m_{e0} \pi} \left(\frac{v_t^2(k^2 - \beta^2)H_{-s}\{k_t r_H, k_t r_L\}}{(\omega - \beta v_z - s\omega_c/\gamma)^2} - \frac{(\omega - \beta v_z)Q_{-s}\{k_t r_H, k_t r_L\}}{\omega - \beta v_z - s\omega_c/\gamma} \right) \quad (5)$$

where N_0 is the number of electrons per unit axial length of the beam; v_t and v_z are, respectively, the transverse and the axial velocities of the electrons in relativistic electron beam;

$$H_{-s}\{k_t r_H, k_t r_L\} = Z_s^2\{k_t r_H\} Z_s'^2\{k_t r_L\}$$

and

$$Q_{-s}\{k_t r_H, k_t r_L\} = 2Z_s^2\{k_t r_H\} Z_s'^2\{k_t r_L\} + 2k_t r_L Z_s\{k_t r_H\} Z_s'\{k_t r_L\} Z_s''\{k_t r_L\}.$$

One may review (5) for the relativistic electron beam in which high transverse velocity (large value of v_t) and near beam harmonic

resonance $\omega - \beta v_z - s\omega_c/\gamma \approx 0$ [7–9]. The first term in right hand side of (5), involves v_t^2 in the numerator and $(\omega - \beta v_z - s\omega_c/\gamma)^2$ in the denominator, obviously dominates over the second term. Therefore, one may write the dispersion relation of a gyro-TWT, retaining only the first term in (5), as

$$k^2 - \beta^2 - k_t^2 = \frac{-\mu_0 |e|^2 N_0 v_t^2 (k^2 - \beta^2) H_{-s}\{k_t r_H, k_t r_L\}}{2\chi\gamma m_{e0} \pi (\omega - \beta v_z - s\omega_c/\gamma)^2},$$

that may be rearranged to write as

$$(k^2 - \beta^2 - k_t^2) \left(\omega - \beta v_z - \frac{s\omega_c}{\gamma} \right)^2 = \frac{-\mu_0 |e|^2 N_0 v_t^2 (k^2 - \beta^2) H_{-s}\{k_t r_H, k_t r_L\}}{2\chi\gamma m_{e0} \pi}. \quad (6)$$

3. GYRO-TWT GAIN EQUATION

In line with the approach earlier used by Pierce [11] to get the gain equation of a conventional TWT, the dispersion relation (6) may be interpreted for the gain equation of a gyro-TWT. For the purpose, one may substitute the axial phase propagation constant for the waveguide-mode $\beta_{mn} = (k^2 - k_t^2)^{1/2}$ and the beam propagation constant parameter $\beta_{e,gyro} = (\omega - s\omega_c/\gamma)/v_z$ into (6), to obtain

$$\beta_{mn}^2 - \beta^2 = \frac{-\mu_0 |e|^2 N_0 v_t^2 (k^2 - \beta^2) H_{-s}\{k_t r_H, k_t r_L\}}{2\chi\gamma m_{e0} \pi (\beta_{e,gyro} - \beta)^2 v_z^2}. \quad (7)$$

The rearranged form of (7) may be written as

$$\frac{(\beta_{mn}^2 - \beta^2) (\beta_{e,gyro} - \beta)^2}{k^2 - \beta^2} = \frac{-\mu_0 |e|^2 N_0 v_t^2 H_{-s}\{k_t r_H, k_t r_L\}}{2\chi\gamma m_{e0} \pi v_z^2}. \quad (8)$$

The fourth degree Equation (8) in β would give four solutions for it. Out of the four, three will be for three forward waves and one for backward wave. A simplified third degree equation, corresponding to three forward wave solutions, may be obtained, as for a conventional TWT formulism (Pierce’s approach [11]) [7–9]. In the present context, one may proceed as follows by letting

$$\beta = \beta_{mn}(1 + j C_{gyro}\delta) \quad (9)$$

and

$$\beta_{e,gyro} = \beta_{mn}(1 + b_{gyro} C_{gyro}), \quad (10)$$

where each of C_{gyro} , δ and b_{gyro} are dimensionless quantities assuming $C_{gyro}\delta \ll 1$ and $b_{gyro} C_{gyro} \ll 1$.

One may square both sides of (9) and rearrange the terms to obtain:

$$\beta_{mn}^2 - \beta^2 = -j 2 \beta_{mn}^2 C_{gyro} \delta (1 + j C_{gyro} \delta / 2). \quad (11)$$

Under the approximation $C_{gyro} \delta \ll 1$, (11) becomes

$$\beta_{mn}^2 - \beta^2 = -j 2 \beta_{mn}^2 C_{gyro} \delta. \quad (12)$$

Further, subtracting (9) from (10) and squaring the resultant relation gives

$$(\beta_{e, gyro} - \beta)^2 = [\beta_{mn} C_{gyro} (b_{gyro} - j\delta)]^2. \quad (13)$$

Here, one may recall the waveguide-mode dispersion relation

$$k^2 - \beta^2 = k_t^2. \quad (14)$$

Now, substituting (12), (13) and (14), into left hand side of (8), one may write

$$\frac{-j 2 \beta_{mn}^4 C_{gyro}^3 \delta (b_{gyro} - j\delta)^2}{k_t^2} = \frac{-\mu_0 |e|^2 N_0 v_t^2 H_{-s}\{k_t r_H, k_t r_L\}}{2\chi\gamma m_{e0}\pi v_z^2}. \quad (15)$$

Further, for involving the beam voltage V_0 in (15), one may obtain an expression for v_z^2 , to be put in (15), in terms of V_0 and the beam pitch factor $\alpha_0 (= v_t/v_z)$. For this, one may first write the relativistic mass factor γ in terms of v_z and v_t , as

$$\gamma = [1 - (v_z^2 + v_t^2)/c^2]^{-1/2}. \quad (16)$$

Other way, γ may be expressed in terms of the beam potential V_0 , by equating the beam potential energy $|e| V_0$ with the relativistic kinetic energy $\gamma m_{e0} c^2 - m_{e0} c^2$, as

$$\gamma = 1 + |e| V_0 / m_{e0} c^2. \quad (17)$$

With the help of (16) and (17), and making use of the relation $\gamma/(\gamma + 1) \approx 1/2$, one may thus obtain

$$v_z^2 \cong 2 |e| V_0 / [\gamma m_{e0} (1 + \alpha_0^2)]. \quad (18)$$

One may substitute v_z^2 from (18) into (15), and put $N_0 = I_0 / (|e| v_z)$, where I_0 is the dc beam current; $v_t = \eta_t c$ and $v_z = \eta_z c$; and $c = (\mu_0 \epsilon_0)^{-1/2}$ in the resulting relation, to obtain

$$\frac{-j 2 \beta_{mn}^4 C_{gyro}^3 \delta (b_{gyro} - j\delta)^2}{k_t^2} = \frac{-(\mu_0 / \epsilon_0)^{1/2} I_0 \eta_t^2 H_{-s}\{k_t r_H, k_t r_L\} (1 + \alpha_0^2)}{4\chi\pi V_0 \eta_z},$$

that may be re-written in simpler form, as

$$j C_{gyro}^3 \delta (b_{gyro} - j\delta)^2 = K_{gyro} I_0 / 4V_0 \quad (19)$$

where

$$K_{gyro} = \frac{(\mu_0/\epsilon_0)^{1/2} \eta_t^2 (1 + \alpha_0^2) k_t^2 H_{-s}\{k_t r_H, k_t r_L\}}{2\chi\pi \beta_{mn}^4 \eta_z}.$$

If one takes, the arbitrarily chosen dimensionless quantity C_{gyro} as $C_{gyro}^3 = K_{gyro} I_0 / 4V_0$ [1–3, 7–9] to be substituted into the left hand side of (19), one obtains the following cubic equation $\delta(jb_{gyro} + \delta)^2 = j$. Further, running parallel to the approach used by Pierce [11] for a conventional TWT, one may then develop the small-signal gain equation of a gyro-TWT as [7–9]:

$$G = A + B_{guide} C_{gyro} N_{gyro, guide}, \tag{20}$$

where A is the lurching loss; B_{guide} is the growth parameter; and $N_{gyro,guide}$ is number of guide wavelength in the interaction length.

4. RESULTS AND DISCUSSION

The field matching technique at the cylindrical interface of discontinuity of the considered structures gives their dispersion relations as presented in beam-absent analysis of the configurations (part-1). The solution of beam-absent dispersion relations (part-1) may be substituted into the Pierce-type gain Equation (20) of the considered structures to obtain the gain in dB for different frequencies. In order to get the gain value for each frequency lying in the passband, one may use a numerical code followed the analysis (Section 3) and developed in MATLAB, in which for the value of phase propagation constant one has to use the numerical code developed on the basis of beam-absent analysis (part-1). Thus, the idea of part-1 and part-2 completes the study.

The gyro-TWT developed successfully so far mostly uses cylindrical waveguide as an interaction structure [6], taking that as a reference author is presenting a comparison study and the possible applicability of the proposed structures as interaction structures. For the purpose of comparison of the devices with considered interaction structures a constant mid-frequency of gain-frequency responses is selected around 35 GHz (electromagnetic atmospheric window for the purpose of communication). The frequency range of gain-frequency response of the circular cylindrical waveguide spreads with all four types of loading; namely, coaxial loading in circular waveguide, annular disc loading in circular waveguide, disc-loading in coaxial waveguide in two configurations; where the coaxial loading spreads the frequency range maximum. Similarly, the device bandwidth broadens with all four types of loading, where improvement in bandwidth is minimum

and maximum for the coaxial loading and disc-loading in circular waveguide, respectively. There is a mild decrease in gain in case of disc-loading in circular waveguide, whereas a visible decrease in gain for the case of disc-loading on coaxial rod. However, there is good and better improvement in gain for the case of coaxial-loading the circular waveguide and annular disc-loading the coaxial waveguide, respectively.

In addition, for the foresaid responses the beam velocity pitch factor takes lower values than that of circular waveguide interaction structure. Although, the gain decreases for the case of disc-loading on coaxial rod, it takes least value of beam velocity pitch factor (Fig. 2). For the constant value of waveguide/envelope radius, the mid-frequency of the gain-frequency response shifts to higher frequency side for all four types of loading. The shifts for all three disc-loaded structures are almost constant and more than that of coaxial-loading the circular waveguide (Fig. 3).

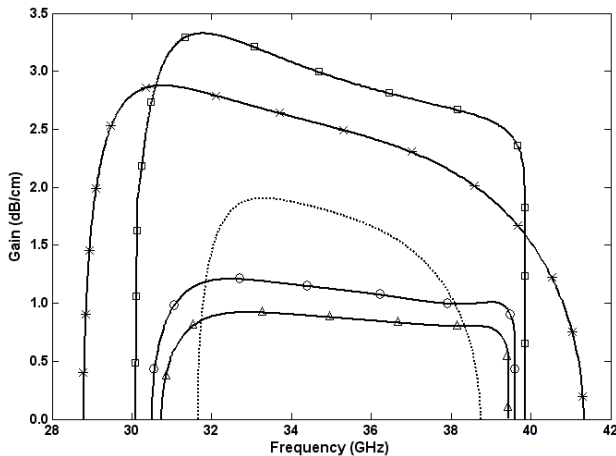


Figure 2. Gain-frequency response of the TE_{01} -mode of circular cylindrical waveguide ($r_W = 5.9$ mm, $\alpha_0 = 0.7$) (broken curve), disc-loaded circular waveguide ($r_W = 8.1$ mm, $\alpha_0 = 0.4$, $r_D/r_W = 0.7$, $L/r_W = 0.6$, $T/r_W = 0.1$) (curve with circles), coaxial waveguide ($r_W = 6.6$ mm, $\alpha_0 = 0.2$, $r_C/r_W = 0.1$) (curve with stars), and disc-loaded-coaxial waveguides with metal discs radially projecting inward from the metallic envelope (Fig. 1(a)) ($r_W = 8.15$ mm, $\alpha_0 = 0.35$, $r_D/r_W = 0.7$, $r_C/r_W = 0.1$, $L/r_W = 0.6$, $T/r_W = 0.1$) (curve with squares) and metal discs radially projecting outward from the coaxial insert (Fig. 1(b)) ($r_W = 8.1$ mm, $\alpha_0 = 0.1$, $r_D/r_W = 0.4$, $r_C/r_W = 0.1$, $L/r_W = 0.6$, $T/r_W = 0.1$) (curve with triangles) taking $s = 1$, $m = 0$, $I_0 = 9$ A, $V_0 = 100$ kV, $B_0/B_g = 0.99$.

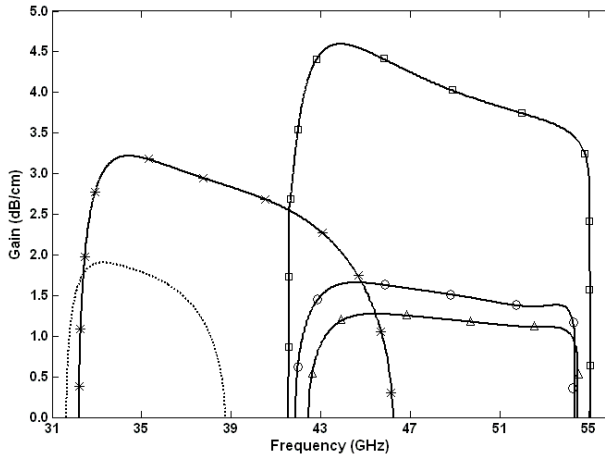


Figure 3. Gain-frequency response of the TE_{01} -mode of circular cylindrical waveguide ($\alpha_0 = 0.7$) (broken curve), disc-loaded circular waveguide ($\alpha_0 = 0.4$, $r_D/r_W = 0.7$, $L/r_W = 0.6$, $T/r_W = 0.1$) (curve with circles), coaxial waveguide ($\alpha_0 = 0.2$, $r_C/r_W = 0.1$) (curve with stars), and disc-loaded-coaxial waveguides with metal discs radially projecting inward from the metallic envelope (Fig. 1(a)) ($\alpha_0 = 0.35$, $r_D/r_W = 0.7$, $r_C/r_W = 0.1$, $L/r_W = 0.6$, $T/r_W = 0.1$) (curve with squares) and metal discs radially projecting outward from the coaxial insert (Fig. 1(b)) ($\alpha_0 = 0.1$, $r_D/r_W = 0.4$, $r_C/r_W = 0.1$, $L/r_W = 0.6$, $T/r_W = 0.1$) (curve with triangles) taking $r_W = 5.9$ mm, $s = 1$, $m = 0$, $I_0 = 9$ A, $V_0 = 100$ kV, $B_0/B_g = 0.99$.

5. CONCLUSION

The possibility of a broadband and high-gain gyro-TWT has been presented in a coaxial-type interaction structure. The gain frequency responses for four different interaction structures in comparison with most common circular waveguide interaction structure of a gyro-TWT have been presented. The disc-loaded-coaxial waveguide with metal discs radially projecting inward from the metallic envelope, which has shown maximum promise for device gain and bandwidth, takes maximum value of waveguide radius among the structures considered. This may subsequently help in thermal management of the device. The shifts to higher mid-frequency value of the gain-frequency responses of the device, developed in considered loadings, suggest the higher frequency operation while assuming the constant waveguide radius in different loadings. The analysis involves many interdependent parameters, each playing actively to mold the performance, therefore, it is required to optimize each of the parameters for an optimum result

as per the need. The author is aware that the large signal analysis would predict a more realistic performance, however, the present small signal analysis would be fruitful for device-developer in settling to the first-cut design of a disc-loaded-coaxial gyro-TWT.

ACKNOWLEDGMENT

The author is thankful to Dr. Lalit Kumar, Director of the Centre, for valuable support and guidance.

APPENDIX A. EVALUATION OF THE DEFINITE INTEGRAL OCCURRING IN THE INEXPLICIT FORM OF GYRO-TWT DISPERSION RELATION

Let us assume

$$I = \int_{r=r_X}^{r_Y} \left(\frac{\partial}{\partial r} (r J_\theta) - \frac{\partial J_r}{\partial \theta} \right) Z_0 \{k_t r\} dr$$

to rewrite the inexplicit from (4) of the dispersion relation of a gyro-TWT, as [7]:

$$(k^2 - \beta^2 - k_t^2) \chi B_{z0} \exp(\omega t - \beta z) = -\mu_0 I. \quad (A1)$$

One may express the azimuthal J_θ and the radial J_r components of RF beam current density in terms of the perturbed part of the electron distribution function f_1 , as

$$\left. \begin{aligned} J_r &= -|e| \int f_1 v_r d^3 p \\ J_\theta &= -|e| \int f_1 v_\theta d^3 p \end{aligned} \right\}$$

$$d^3 p = dp_t p_t d\phi dp_z \text{ (volume element in momentum space)}$$

In the real-space polar coordinates (r, θ) , the radial v_r and the azimuthal v_θ electron velocities, are related to the corresponding quantities in the momentum-space polar coordinates (p_t, ϕ) , as (Fig. A1):

$$\begin{aligned} v_r &= v_t \cos(\phi - \theta) = p_t / (\gamma m_{eo}) \cos(\phi - \theta) \\ v_\theta &= v_t \sin(\phi - \theta) = p_t / (\gamma m_{eo}) \sin(\phi - \theta). \end{aligned}$$

Hence, I involved in the right hand side of (A1) is expressed, in terms of f_1 , as [6, 7]:

$$I = k_t |e| \int_{r=r_X}^{r_Y} \int_{p_t=0}^{\infty} \int_{p_z=0}^{\infty} \int_{\phi=0}^{2\pi} \exp j\nu(\theta_H - \theta) \sum_{h=-\infty}^{\infty} Z'_h \{k_t r_L\} Z_{\nu+h} \{k_t r_H\}$$

$$\times \left[\exp -jh \left(\frac{\pi}{2} - \theta_H + \phi \right) \right] \frac{rp_t^2}{\gamma m_{e0}} f_1 dr dp_t dp_z d\phi. \quad (A2)$$

In order to obtain I in the form of (A2), one has to take the azimuthal component of current density $J_\theta = 0$ both at $r = r_X$ and $r = r_Y$ (in view of the location of the thin hollow beam considered away from both $r = r_X$ and $r = r_Y$). Also, one has to make use of the recurrence relation of Bessel function as used proceeding (2), as well as Graf's addition theorem of Bessel function [7]

$$\exp(\pm i m \theta_1) Z_m\{x_1\} = \sum_{p=-\infty}^{+\infty} \exp(\pm i p \theta_2) Z_{m+p}\{x_2\} Z_p\{x_3\}. \quad (A3)$$

For the present case, one has to take, in (A3), $x_1 = k_t r$, $x_2 = k_t r_H$ and $x_3 = k_t r_L$, so that one may now express a function of r as independent of r but as a function of r_L and r_H , as follows:

$$\begin{aligned} & Z_{\nu-1}\{k_t r\} \exp j(\phi - \theta) + Z_{\nu+1}\{k_t r\} \exp[-j(\phi - \theta)] \\ &= 2j \exp j\nu(\theta_H - \theta) \sum_{h=-\infty}^{\infty} Z'_h\{k_t r_L\} Z_{\nu+h}\{k_t r_H\} \exp[-jh(\pi/2 - \theta_H + \phi)], \end{aligned}$$

where h is an integer.

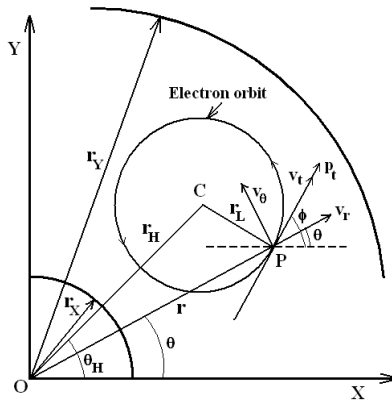


Figure A1. Projection of the electron orbit on the guide cross-sectional plane (X - Y) showing the centre of the guide (O), the guiding centre (C) of the gyrating electron, the real-space coordinates (r_H, θ_H) of the guiding centre, and the real-space (r, θ) and momentum-space (p_t, ϕ) coordinates of the instantaneous position (P) of the gyrating electron (after [7]).

The relativistic Vlasov equation [7–9, 15], introduced later, is solved for f_1 in terms of the equilibrium or unperturbed part of electron distribution function f_0 (the form of which is assigned later), as [7]:

$$f_1 = \frac{|e| B_0}{k_t} \exp j(\omega t - \beta z) \exp(-j\nu\theta_H) \\ \times \left[(\omega - \beta\nu_z) \frac{\partial f_0}{\partial p_t} + \nu_t \beta \frac{\partial f_0}{\partial p_z} \right] \sum_{p=-\infty}^{\infty} \frac{Z_{\nu+p}\{k_t r_H\} Z'_p\{k_t r_L\}}{\omega - \beta\nu_z + p\omega_c/\gamma} \\ \times \exp[jp(\pi/2 - \theta_H + \phi)]. \quad (\text{A4})$$

Hence, I given by (A2) can be expressed, in terms of f_0 , as [7]:

$$I = k_t |e| \exp j\nu(\theta_H - \theta) \int_{r=r_X}^{r_Y} \int_{p_t=0}^{\infty} \int_{p_z=-\infty}^{\infty} \int_{\phi=0}^{2\pi} \sum_{h=-\infty}^{\infty} \sum_{p=-\infty}^{\infty} Z'_h\{k_t r_L\} \\ \times Z_{\nu+h}\{k_t r_H\} \frac{r p_t^2 |e| B_{z0}}{\gamma m_{e0} k_t} \exp j(\omega t - \beta z) \exp(-j\nu\theta_H) \\ \times \left((\omega - \beta\nu_z) \frac{\partial f_0}{\partial p_t} + \nu_t \beta \frac{\partial f_0}{\partial p_z} \right) \left(\frac{Z_{\nu+p}\{k_t r_H\} Z'_p\{k_t r_L\}}{\omega - \beta\nu_z + p\omega_c/\gamma} \right) \\ \times \exp jp \left(\frac{\pi}{2} - \theta_H + \phi \right) dr dp_t dp_z d\phi. \quad (\text{A5})$$

The relativistic Vlasov equation [15], from which to obtain the expression (A4) for f_1 , may be obtained as [3, 7–9]:

$$\left(\frac{\partial}{\partial t} + \frac{p}{\gamma m_{e0}} \cdot \nabla - |e| (E + v \times B) \cdot \nabla_p \right) f_1 = 0, \quad (\text{A6})$$

where $f_1(r, p, t)$ is the perturbed part of electron distribution in the phase space (r, p) ; ∇f_1 is the gradient of f_1 in the physical space; and $\nabla_p f_1$ is its gradient in momentum space. For making the solution process for f_1 simple, the higher-order terms of (A6) are ignored. Along the unperturbed trajectory, (A6) involving the partial time derivative of f_1 simplifies to one involving the complete time derivative as [7]:

$$\frac{df_1}{dt} = |e| (E_1 + v \times B_1) \cdot \nabla_p f_0, \quad (\text{A7})$$

which involves only time (t) variable, and gives the rate of change of the distribution function as observed on the electron trajectory [7–9, 15]. In order to get the solution for f_1 , the time derivative of f_1 (A7) is integrated between a time t and a time before the electrons enter the RF fields which may be set as $-\infty$, that is, a time large in magnitude compared to any time at frequencies of interest. Further, one has to

use the recurrence relations for Bessel function, as used preceding (2) and Graf's addition theorem of Bessel function, as used following (A2), to get f_1 as given in (A4), [7].

Now, a function is assigned to f_0 (say) considering a beam of zero guiding centre spread, in terms of the number of electrons per unit axial interaction length N_0 , the Dirac-delta function with reference to the hollow beam radius r_H having equilibrium value r_{H0} , and the momentum distribution function

$$g\{p_t, p_z\} = \frac{1}{2\pi p_t} \delta\{p_t - p_{t0}\} \delta\{p_z - p_{z0}\},$$

as:

$$f_0 = \frac{N_0}{2\pi r} \delta\{r_H - r_{H0}\} \frac{1}{2\pi p_t} \delta\{p_t - p_{t0}\} \delta\{p_z - p_{z0}\}, \quad (A8)$$

where p_z and p_t are the axial and transverse electron momenta with their equilibrium values p_{z0} and p_{t0} , respectively. The function f_0 from (A8) is substituted into the integral I given by (A5), and then the latter substituted in (A1), to yield the dispersion relation, as:

$$k^2 - \beta^2 - k_t^2 = -\frac{\mu_0 N_0 |e|^2}{\chi} \int_{p_t=0}^{\infty} \int_{p_t=0}^{\infty} \sum_{p=-\infty}^{\infty} \left(\frac{v_t^2 (k^2 - \beta^2) H_{\nu,p}\{k_t r_H, k_t r_L\}}{(\omega - \beta v_z + p \omega_c / \gamma)^2} - \frac{(\omega - \beta v_z) Q_{\nu,p}\{k_t r_H, k_t r_L\}}{\omega - \beta v_z + p \omega_c / \gamma} \right) \frac{p_t \delta\{p_t - p_{t0}\} \delta\{p_z - p_{z0}\}}{\gamma m_{e0} 2\pi p_t} dp_t dp_z \quad (A9)$$

where

$$\eta_t = v_t / c = p_t / \gamma m_{e0} c$$

$$H_{\nu,p} = Z_{\nu+p}^2\{k_t r_H\} Z_p'^2\{k_t r_L\}$$

and

$$Q_{\nu,p} = 2H_{\nu,p} + 2k_t r_L Z_{\nu+p}^2\{k_t r_H\} Z_p'\{k_t r_L\} Z_p''\{k_t r_L\}.$$

Under cyclotron resonance condition, putting $(\omega - \beta v_z - s \omega_c / \gamma) \rightarrow 0$ ($\beta \approx \beta_{mn}$) in the dispersion relation (A9), where now the terms in the summation corresponding to $p \neq -s$ will become negligibly small as compared to the remaining terms (corresponding to $p = -s$), therefore, retaining the terms corresponding to $p = -s$, one may write (A9), as:

$$k^2 - \beta^2 - k_t^2 = -\frac{\mu_0 N_0 |e|^2}{\chi} \int_{p_t=0}^{\infty} \int_{p_t=0}^{\infty} \left(\frac{v_t^2 (k^2 - \beta^2) H_{\nu,-s}\{k_t r_H, k_t r_L\}}{(\omega - \beta v_z - s \omega_c / \gamma)^2} - \frac{(\omega - \beta v_z) Q_{\nu,-s}\{k_t r_H, k_t r_L\}}{\omega - \beta v_z - s \omega_c / \gamma} \right) \frac{p_t \delta\{p_t - p_{t0}\} \delta\{p_z - p_{z0}\}}{\gamma m_{e0} 2\pi p_t} dp_t dp_z. \quad (A10)$$

The integral in (A10) may then be evaluated using the unit-impulse property of Dirac-Delta function, that modifies (A10) as:

$$k^2 - \beta^2 - k_t^2 = \frac{-\mu_0 |e|^2 N_0}{2\chi\gamma m_{e0}\pi} \left(\frac{v_t^2(k^2 - \beta^2)H_{\nu,-s}\{k_t r_H, k_t r_L\}}{(\omega - \beta v_z - s\omega_c/\gamma)^2} - \frac{(\omega - \beta v_z)Q_{\nu,-s}\{k_t r_H, k_t r_L\}}{\omega - \beta v_z - s\omega_c/\gamma} \right) \quad (\text{A11})$$

where

$$H_{\nu,-s}\{k_t r_H, k_t r_L\} = Z_{\nu,-s}^2\{k_t r_H\} Z'_{-s}^2\{k_t r_L\} \quad (\text{A12})$$

and

$$Q_{\nu,-s}\{k_t r_H, k_t r_L\} = 2Z_{\nu,-s}^2\{k_t r_H\} Z'_{-s}^2\{k_t r_L\} + 2k_t r_L Z_{\nu,-s}\{k_t r_H\} Z'_{-s}\{k_t r_L\} Z''_{-s}\{k_t r_L\}. \quad (\text{A13})$$

The dispersion relation (A11), which is valid for all the TE modes, can be read for azimuthally symmetric TE mode by substituting $\nu = 0$ in (A11) as:

$$k^2 - \beta^2 - k_t^2 = \frac{-\mu_0 |e|^2 N_0}{2\chi\gamma m_{e0}\pi} \left(\frac{v_t^2(k^2 - \beta^2)H_{-s}\{k_t r_H, k_t r_L\}}{(\omega - \beta v_z - s\omega_c/\gamma)^2} - \frac{(\omega - \beta v_z)Q_{-s}\{k_t r_H, k_t r_L\}}{\omega - \beta v_z - s\omega_c/\gamma} \right) \quad (\text{A14})$$

where $H_{-s}\{k_t r_H, k_t r_L\}$ and $Q_{-s}\{k_t r_H, k_t r_L\}$, in view of the relations $Z_{-n}\{x\} = (-1)^n Z_n\{x\}$ and $Z'_{-n}\{x\} = (-1)^n Z'_n\{x\}$ [14], can be read from (A12) and (A13), respectively, as

$$H_{-s}\{k_t r_H, k_t r_L\} = Z_s^2\{k_t r_H\} Z_s'^2\{k_t r_L\}$$

and

$$Q_{-s}\{k_t r_H, k_t r_L\} = 2Z_s^2\{k_t r_H\} Z_s'^2\{k_t r_L\} + 2k_t r_L Z_s\{k_t r_H\} Z_s'\{k_t r_L\} Z_s''\{k_t r_L\}.$$

The dispersion relation (A14) is used as (5) in Section 3.

REFERENCES

1. Rao, S. J., P. K. Jain, and B. N. Basu, "Broadbanding of gyro-TWT by dispersion shaping through dielectric loading" *IEEE Trans. Electron Dev. Lett.*, Vol. 43, No. 12, 2290–2299, Dec. 1996.
2. Rao, S. J., P. K. Jain, and B. N. Basu, "Two-stage dielectric-loading for broadbanding a gyro-TWT," *IEEE Electron Dev. Lett.*, Vol. 17, No. 6, 303–305, Jun. 1996.

3. Rao, S. J., P. K. Jain, and B. N. Basu, "Hybrid-mode helix-loading effects on gyro-travelling-wave tubes," *Int. J. Electronics*, Vol. 82, 663–675, 1997.
4. Singh, G., "Analytical study of the interaction structure of vane-loaded gyro-traveling wave tube amplifier," *Progress In Electromagnetics Research B*, Vol. 4, 41–66, 2008.
5. Kesari, V., P. K. Jain, and B. N. Basu, "Analysis of a circular waveguide loaded with thick annular metal discs for wideband gyro-TWTs," *IEEE Trans. Plasma Sci.*, Vol. 33, No. 4, 1358–1365, Aug. 2005.
6. Kesari, V., *Analysis of Disc-loaded Circular Waveguides for Wideband Gyro-TWTs*, LAP-Lambert Academic Publishing AG & Co., Germany (ISBN: 978-3-8383-1145-6), 2009.
7. Basu, B. N., *Electromagnetic Theory and Applications in Beam-Wave Electronics*, World Scientific, Singapore, 1996.
8. Sangster, A. J., "Small-signal analysis of the travelling-wave gyrotron using Pierce parameters," *Proc. IEE*, Vol. 127, 45–52, 1980.
9. Sangster, A. J., "Small-signal bandwidth characteristics of a travelling-wave gyrotron amplifier," *Int. J. Electronics*, Vol. 51, 583–594, 1981.
10. Malek, F., "The analytical design of a folded waveguide traveling wave tube and small signal gain analysis using Madey's theorem," *Progress In Electromagnetics Research*, Vol. 98, 137–162, 2009.
11. Pierce, J. R., *Traveling-Wave Tubes*, D. Van Nostrand, New Jersey, 1950.
12. Zhu, Z. J., B. F. Jia, and D. M. Wan, "Efficiency improvement of helix traveling-wave tube," *Journal of Electromagnetic Waves and Applications*, Vol. 22, No. 13, 1747–1756, 2008.
13. Duan, Z. Y., Y. B. Gong, Y. Y. Wei, W. X. Wang, B.-I. Wu, and J. A. Kong, "Efficiency improvement of broadband helix traveling wave tubes using hybrid phase velocity tapering model," *Journal of Electromagnetic Waves and Applications*, Vol. 22, No. 7, 1013–1023, 2008.
14. Waldron, R. A., *Theory of Guided Electromagnetic Waves*, Van Nostrand Reinhold, London, 1970.
15. Vlasov, A. A., "The vibrational properties of an electron gas," *Zh. Eksp. Teor. Fiz.*, Vol. 8, 291–318, 1938.